Two-Dimensional Turbulence with Local Interactions: Statistics of the Condensate

Anton Svirsky[1], Corentin Herbert[2], and Anna Frishman[1,*]

[1]*Physics Department, Technion Israel Institute of Technology, 32000 Haifa, Israel*
[2]*ENS de Lyon, CNRS, Laboratoire de Physique, F-69342 Lyon, France*

Two-dimensional turbulence self-organizes through a process of energy accumulation at large scales, forming a coherent flow termed a condensate. We study the condensate in a model with local dynamics, the large-scale quasigeostrophic equation, observed here for the first time. We obtain analytical results for the mean flow and the two-point, second-order correlation functions, and validate them numerically. The condensate state requires partiy + time-reversal symmetry breaking. We demonstrate distinct universal mechanisms for the even and odd correlators under this symmetry. We find that the model locality is imprinted in the small scale dynamics, which the condensate spatially confines.

Introduction.—Understanding the interactions between turbulent fluctuations and a mean flow is a central problem in fluid mechanics. Such interactions usually prevent a prediction of the mean flow due to their nonlinear nature. Recently, some progress was made in this direction for two-dimensional turbulence [1,2]. In this case, the mean flow spontaneously emerges from small-scale fluctuations in an out-of-equilibrium process of self-organization. The underlying mechanism is that of an inverse transfer of energy—from small to large scales, leading to the accumulation of energy at large scales and the establishment of a system-size mean flow termed a condensate [3].

Two-dimensional flow minimalistically encapsulates the main dynamical constraints imposed by rotation and density stratification, encountered in nature or in laboratory experiments [4]. In fact, a cornerstone of the theory of large-scale dynamics of geophysical flows, including the formation of coherent structures such as jets and vortices, is the quasigeostrophic (QG) approximation [5], which shares the same fundamental structure as two-dimensional flow. However, a general understanding of the feedback between such structures and turbulence within the QG framework is currently lacking.

In QG, there is a typical scale for the range of fluid elements interactions, called the Rossby radius of deformation L_d. The special cases which have been studied in detail so far correspond to dynamics at scales much smaller than L_d: the vortex condensate in two-dimensional incompressible Navier-Stokes (2DNS) [1,2,6–10], and jets in the presence of strong differential rotation (β effect) [11–15]. Here, we address the opposite limit, of scales much larger than L_d (without differential rotation): the large-scale quasigeostrophic (LQG) equation [16]. We observe the condensate regime in LQG for the first time in numerical simulations, and provide a detailed theoretical picture of the mean-flow–turbulence interactions. Although the flow is turbulent and the mean flow is sustained due to nonlinear interactions, we show that the statistics can be captured within a perturbative approach, the quasilinear approximation [17]. This reinforces the relevance of the approach for low-order turbulence statistics in the presence of a strong mean flow [1,2]. While in 2DNS fluid-element interactions are long range, in LQG they are local. Comparing the two cases, our work sheds light on the influence of the range of interactions on the condensate state. Indeed, we show that the statistics at large scales are determined by universal underlying mechanisms. On the other hand, at small scales we find that the locality of interactions has a dramatic influence, with small-scale fluxes and dissipation suppressed in regions where the mean flow is strong.

Framework.—Both the LQG equation and 2DNS can be derived as limiting cases of the shallow water quasigeostrophic (SWQG) equation. This is an idealized model widely used for flows in the atmosphere and oceans [5], and for magnetically confined plasmas [18]. In the geophysical context, it captures the dynamics of the free surface of a rapidly rotating shallow fluid layer under the influence of gravity. The inviscid SWQG equation reads $\partial_t q + \mathbf{v} \cdot \boldsymbol{\nabla} q = \partial_t q + J(\psi, q) = 0$, where $q = (\nabla^2 - L_d^{-2})\psi$, is the potential vorticity, $J(\psi, q) = \partial_x \psi \partial_y q - \partial_y \psi \partial_x q$, and ψ is the stream function related to the velocity field by $\mathbf{v} = \hat{\mathbf{z}} \times \boldsymbol{\nabla}\psi$. The flow is assumed to be in geostrophic balance. Thus, ψ is proportional to the deviation of the fluid layer height from its mean. The system has L_d as a characteristic length scale, determining the range of influence of a height perturbation. If the domain size $L \ll L_d$ then every fluid element will influence every other, and the flow will become incompressible, giving the 2DNS. The opposite limit $L_d/L \to 0$ giving LQG (which can be made consistent with the SWQG approximation [19]), corresponds to a very rapidly rotating fluid where surface perturbations remain completely localized. The dynamics become slow in this

limit, requiring the rescaling of time as $\tau = t(L_d/L)^2$ (and ψ accordingly), resulting in the LQG equation

$$\partial_\tau \psi + \boldsymbol{v}^\omega \cdot \boldsymbol{\nabla}\psi = \partial_\tau \psi + J(\omega, \psi) = f + \alpha\nabla^2\psi - \nu(-\nabla^2)^p\psi, \quad (1)$$

where we defined an effective velocity $\boldsymbol{v}^\omega = \hat{z} \times \boldsymbol{\nabla}\omega$, f is a forcing term, and the last two terms are dissipative—a viscous term referred to as drag in the following, and a hyperviscosity. The former provides the dominant dissipation mechanism at large scales, while the latter will dominate at small scales. The inviscid invariants of (1) are the kinetic energy $Z = \frac{1}{2}\int(\nabla\psi)^2 d^2x = \frac{1}{2}\int v^2 d^2x$ and all moments of ψ, in particular the potential energy $E = \frac{1}{2}\int\psi^2 d^2x$. The existence of two positive quadratic invariants results in the inverse cascade of E and a direct cascade (from large to small scales) of Z [20].

The LQG advection equation is similar to 2DNS but with the roles of the vorticity $\omega = \nabla^2\psi$ and the stream function reversed. Indeed, LQG and 2DNS are part of a class of active scalar equations where a scalar q is advected by a velocity with stream function ϕ, and $q_k = |k|^m\phi_k$ [21], m controlling the range of the dynamics [22]. For 2DNS, $m = 2$ and the dynamics is long range. For LQG $m = -2$, so that the advecting velocity is determined by active scalar gradients, making the dynamics local.

Simulations.—Direct numerical simulations (DNS) are performed by integrating (1) using the Dedalus framework [23]. Simulating in a doubly periodic box of dimensions $L \equiv L_y = 2L_x = 2\pi$, we enforce the formation of a jet-type condensate by breaking the symmetry between the x and y directions [24,25]. We use a spatial resolution of 64×128, a white-in-time forcing with characteristic length scale $l_f = 2\pi/13$, hyperviscosity with $p = 7$ and $\nu = 7.3 \times 10^{-19}$ and take $\alpha = (0.5, 1, 2) \times 10^{-3}$. Condensation of E at large scales requires a slow dissipation rate compared to the eddy-turnover time at the box scale, amounting to the condition $\delta \equiv \alpha(L^2/\epsilon)^{1/3} \ll 1$, where $\epsilon = \langle f\psi \rangle$ is the energy injection rate. Additional simulation details, including for DNS with other parameters, are in [19].

The steady state condensate takes the form of two alternating jets along the short side (x direction) of the domain, as demonstrated in Fig. 1. Here, the jet structure is selected by the domain geometry, unlike in β-plane turbulence. Between the jets, there are two small vortices, similarly to what was found in 2DNS [25].

Mean flow.—We now set out to obtain a statistical description of the steady state LQG jet condensate. We start by decomposing the flow into the mean $\Psi = \langle \psi \rangle$ and fluctuations $\psi' = \psi - \Psi$. We will focus on the jet region, where the flow is statistically homogeneous in x, and the mean flow depends on y only. In particular, the mean flow is in the x direction: $U = -\partial_y\Psi$. In the steady state, averaging (1) and neglecting the influence of hyperviscosity at large scales we obtain
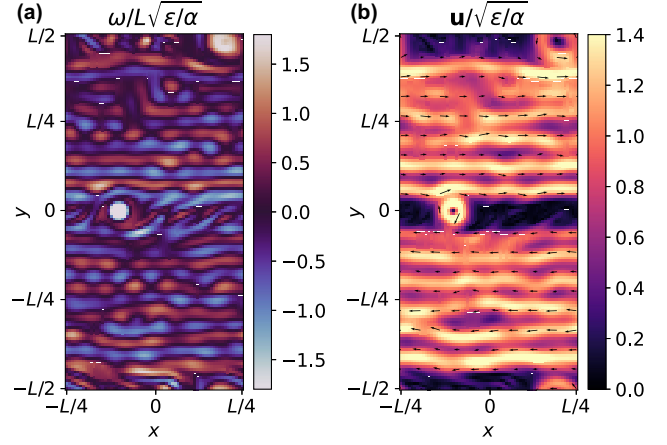

FIG. 1. LQG jet condensate in a periodic, rectangular box with $\delta = 0.052$. (a) Vorticity snapshot $\omega = \nabla^2\psi$ and (b) velocity snapshot $\boldsymbol{v} = \hat{z} \times \boldsymbol{\nabla}\psi$.

$$\partial_y[\langle v_y^{\omega\prime}\psi' \rangle - \alpha\partial_y\Psi] = 0, \quad (2)$$

where we have used that $V_y^\omega = \partial_x\langle\omega\rangle = 0$. As mentioned before, ψ is proportional to the layer height, thus (2) can be interpreted as a mass balance and $\langle v_y^{\omega\prime}\psi' \rangle$ as the turbulent mass flux, analogously to the momentum flux or Reynolds stress in 2DNS. We note that a constant nonzero total flux is inconsistent with the symmetries of our system, as there is no preferred direction aside from the one imposed by the emerging mean flow, giving

$$\langle v_y^{\omega\prime}\psi' \rangle = \alpha\partial_y\Psi. \quad (3)$$

Next, we obtain the potential energy balance of the mean flow by multiplying (1) by Ψ and averaging

$$\partial_y[\Psi\langle v_y^{\omega\prime}\psi'\rangle - \alpha\Psi\partial_y\Psi] = \langle v_y^{\omega\prime}\psi'\rangle\partial_y\Psi - \alpha(\partial_y\Psi)^2. \quad (4)$$

Similarly, we obtain the potential energy balance of fluctuations by multiplying (1) by ψ' and averaging, giving

$$\partial_y\left[\left\langle v_y^{\omega\prime}\frac{\psi'^2}{2}\right\rangle\right] = \epsilon - \langle v_y^{\omega\prime}\psi'\rangle\partial_y\Psi. \quad (5)$$

In writing (5) we have neglected the dissipation of potential energy by fluctuations, since the development of the condensate implies dissipation by fluctuations is inefficient and thus small. Equations (4) and (5) reflect the flow of potential energy in the system, where the interaction term $\langle v_y^{\omega\prime}\psi'\rangle\partial_y\Psi = -U\langle v_y^{\omega\prime}\psi'\rangle$ controls the out-of-equilibrium transfer of energy between the fluctuations and the mean flow. The inverse nature of potential energy transfer in this system implies that it goes *from* the

fluctuations *to* the mean flow. This requires mass flux up the gradient of the mean height: $\langle \psi' v^{\omega'} \rangle \cdot \nabla \Psi > 0$.

Because of relation (3) the left hand side of Eq. (4), corresponding to the spatial flux of mean potential energy Ψ^2, vanishes. Thus, here unlike in 2DNS [1], all the energy input from the fluctuations is dissipated locally by the mean flow. Note that the transfer of potential energy to the mean flow cannot be the dominant process in regions where $\partial_y \Psi = -U \approx 0$ since $\langle v_y^{\omega'} \psi' \rangle \partial_y \Psi$ is small there. For jets in a periodic domain there always must be such a region as $\int \nabla \Psi d^2 x = 0$ identically.

Finally, to close the system of equations we assume that interactions with the mean flow are much faster than nonlinear interactions between fluctuations, $|\langle v_y^{\omega'} \psi' \rangle \partial_y \Psi| \gg |\langle \psi' v^{\omega'} \cdot \nabla \psi' \rangle|$, justified by the development of a strong condensate for $\delta \ll 1$. This is called the quasilinear approximation, which has a long history [17], and was recently successfully used in a similar context for 2DNS [1]. Unlike 2DNS, in LQG the dynamics are local (e.g., no pressure term), and thus so is the analysis, obviating the need for further approximations.

Using (3) together with (5) in the quasilinear approximation gives the leading order solution

$$\partial_y \Psi = -U = \pm \sqrt{\frac{\epsilon}{\alpha}}, \qquad (6)$$

$$\langle \psi' v_y^{\omega'} \rangle = \pm \sqrt{\epsilon \alpha}, \qquad (7)$$

implying a flat mean velocity profile U (and mass flux) for each of the jets. We compare these predictions to results from DNS in Fig. 2. For the averaging procedure, after reaching steady state, we perform a temporal (over ~1000

large scale turnover time) as well as a spatial average along the x axis, utilizing the homogeneity of the system. For the mean velocity profile, good agreement with (6) can be seen in Fig. 2(a), demonstrating convergence to the leading order prediction with decreasing δ. The main difference between DNS and the theoretical prediction is the oscillations of the jet velocity seen in DNS (see also Fig. 1), which persist after averaging over long times. They appear to be a subleading correction to the mean flow profile U (controlled by a small parameter other than δ), not captured at leading order. The mass flux $\langle \psi' v_y^{\omega'} \rangle$ is also computed from DNS, shown in Fig. 2(b). It fluctuates about the theoretical prediction, due to rapid fluctuations of $v_y^{\omega'}$ requiring additional statistics for convergence. Still, the sign of the mass flux always matches the sign of $\partial_y \Psi$ (in the jet region), as is necessary for the inverse transfer.

Two-point correlation function.—Having obtained the mean flow profile, we now examine the two-point (single-time) correlation function $\langle \psi_1' \psi_2' \rangle \equiv \langle \psi'(\mathbf{r_1}) \psi'(\mathbf{r_2}) \rangle$ where $\mathbf{r_i} = (x_i, y_i)$. We obtain an equation for $\langle \psi_1' \psi_2' \rangle$ at leading order in perturbation theory from (1), neglecting dissipation of the fluctuations, using the statistical homogeneity in x, and the quasilinear approximation to neglect higher order moments [19]. In addition, we use that from Eq. (6), $V_x^\omega = 0$ at leading order. We thus get

$$[\mathcal{L}_1 + \mathcal{L}_2] \langle \psi_1' \psi_2' \rangle = 2\epsilon \Phi_{12}, \qquad (8)$$

where the operator $\mathcal{L}_i = \partial_{y_i} \Psi(y_i) \nabla^2 \partial_{y_i}$ (no summation is implied here) and $\langle f(\mathbf{r_1}, t) f(\mathbf{r_2}, t') \rangle = 2\epsilon \Phi_{12} \delta(t - t')$ is the force two-point correlation function with $\Phi_{12} \equiv \Phi(\Delta x / l_f, \Delta y / l_f)$. Using the mean profile Eq. (6), this equation reads

$$\partial_{y_+} \partial_{y_-} \partial_{x_1} \langle \psi_1' \psi_2' \rangle = 2\sqrt{\epsilon \alpha} \Phi_{12}, \qquad (9)$$

where we have defined the variables $y_+ = [(y_1 + y_2)/2]$ and $y_- = \Delta y / 2 = [(y_1 - y_2)/2]$. Integrating (9) we get

$$\langle \psi_1' \psi_2' \rangle = C(\Delta x, \Delta y) + 2y_+ \sqrt{\alpha \epsilon} l_f^2 \int_0^{\frac{\Delta x}{l_f}} dz \int_0^{\frac{\Delta y}{2l_f}} dz' \tilde{\Phi}(z, z'), \qquad (10)$$

with $\tilde{\Phi}(x, y) = \Phi(x, y) - \hat{\Phi}(k_x = 0, y) - \hat{\Phi}(x, k_y = 0)$, subtracting the contribution to the forcing from $k_x = 0$ and $k_y = 0$ modes [19]. The second term in (10) is the inhomogeneous solution to Eq. (9), due to a balance between the forcing and the mean flow. The first term, $C(\Delta x, \Delta y)$, is a homogeneous solution of (10), i.e., a zero mode of the advection operator $\mathcal{L}_1 + \mathcal{L}_2 = \partial_{y_+} \partial_{y_-} \partial_{x_1}$. This family of zero modes is chosen assuming decaying correlations with $\Delta y \to L/2$, and using the result from DNS that the variance $\langle (\psi')^2 \rangle$ is constant in the jet region [19]. Deriving the functional form and amplitude of the zero modes is beyond the scope of this work. Empirically, our DNS results [19]

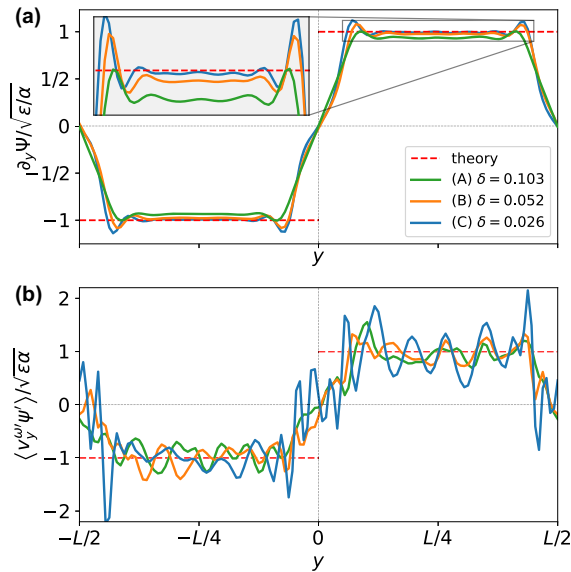

FIG. 2. (a) Horizontal velocity profile $\partial_y \Psi$, dashed line is the prediction (6); (b) mass flux $\langle v_y^{\omega'} \psi' \rangle$, dashed line is the prediction (7).

point to the scaling $\langle u'^2 \rangle = -\partial^2_{\Delta y} C|_{(0,0)} \sim (\epsilon L)^{2/3} \delta^{-1/2}$ and $\langle v'^2 \rangle = -\partial^2_{\Delta x} C|_{(0,0)} \sim (\epsilon L)^{2/3} \delta^{1/4}$, while from Eq. (7) the off-diagonal term $\langle u'v' \rangle = (\epsilon L)^{2/3}(y/L)\delta^{1/2}$. Thus, the perturbation theory is indeed consistent, at most $\langle u'^2 \rangle / U^2 \sim \delta^{1/2} \ll 1$.

PT symmetry breaking.—The condensate state owes its existence to out-of-equilibrium fluxes which break time-reversal symmetry. On the level of single time correlators such symmetry breaking will manifest itself through a combined parity + time (PT) reversal, $x \to -x$ and $t \to -t$, breaking. Indeed, the inviscid LQG dynamics with a homogeneous in x mean flow is statistically invariant under PT. However, the mass flux $\langle \psi' v_y^{\omega'} \rangle$ (responsible for the inverse transfer of energy) is odd under this symmetry and can be nonzero only if it is broken.

We propose that even and odd under PT correlators are determined through different mechanisms, reflected in the decomposition of the two-point correlator (10) into, respectively, the zero modes and inhomogeneous solution. The inhomogeneous solution is determined by a balance between the forcing, which breaks time reversal symmetry, and the mean flow, which breaks parity (but preserves PT). The homogeneous solution, on the other hand, is insensitive to the forcing and instead is a zero mode of the advection operator $\mathcal{L}_1 + \mathcal{L}_2$. A similar structure was inferred in 2DNS [2,9,10].

The inhomogeneous term in (10) is indeed odd under PT: it changes sign under reflection $x \to -x$ (so that $\Delta x \to -\Delta x$) and, being a single-time quantity, does not explicitly depend on time. We propose that it fully determines odd correlators. The mass flux $\langle \psi' v_y^{\omega'} \rangle$ can indeed be directly computed from it, in agreement with (7) [19]. The limit of large scale separation $L/l_f \gg 1$ is interesting to consider at this point, as in this limit we expect universal behavior, independent of forcing details. This is manifested in Eq. (10): the influence of the inhomogeneous term becomes limited to separations $\Delta x, \Delta y \lesssim l_f$, meaning that its main role becomes to determine single-point (odd) correlation functions [19].

Turning to even-under-PT correlators, if they are determined by zero modes then those should be even under PT, implying $C(-\Delta x, \Delta y) = C(\Delta x, \Delta y)$. We verify this property, as well as that the even part of $\langle \psi'_1 \psi'_2 \rangle$ is independent of y_+ in the jet region, as expected for the zero modes, in [19].

Arrest of the direct cascade.—The condensate necessarily coexists with a direct cascade to small scales of a second inviscidly conserved quantity—the kinetic energy in LQG. As the direct cascade involves scales from the forcing scale and smaller, we generally expect the mean flow to have a negligible effect on it. This is indeed the case in 2DNS [25] where the direct cascade of enstrophy (squared vorticity) remains homogeneous and isotropic, as reflected in an essentially spatially uniform enstrophy
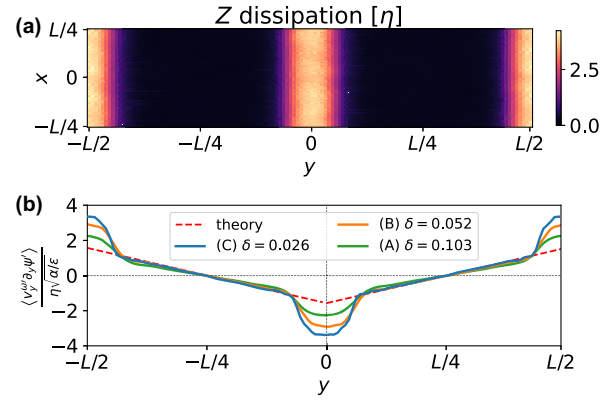

FIG. 3. (a) Mean kinetic energy dissipation normalized by η; (b) The term $\langle v_y^{\omega'} v_x' \rangle$ as measured from DNS, the theoretical prediction (14) is marked by the dashed line.

dissipation rate. Surprisingly, we find this is not the case in LQG, as seen in Fig. 3(a): the kinetic energy dissipation is concentrated in regions in between the jets, being close to zero elsewhere. To explain this inhomogeneity we turn to the kinetic energy balance, obtained by multiplying the derivative ∂_i of (1) by $\partial_i \psi'$ and averaging. In the steady state, the balance of kinetic energy for the fluctuations reads [19]:

$$\partial_y[J'_y + I'_D] = \eta - D' + T, \tag{11}$$

where η is the kinetic energy injection rate, I'_D and D' originate from the viscous terms and are the respective flux and dissipation rate, $T = \partial_y U \partial_y \langle v_y^{\omega'} \psi' \rangle$ is a transfer term between the mean flow and the fluctuations, and J'_y is a spatial kinetic energy flux given by

$$J'_y = U \langle v_y^{\omega'} u' \rangle + \langle \partial_y \psi' \mathbf{v}^{\omega'} \cdot \nabla \psi' \rangle - \langle \omega' v_y^{\omega'} \psi' \rangle. \tag{12}$$

The transfer term T both here and in 2DNS can be estimated to generically be much smaller than the injection rate η [19]. It identically vanishes for the leading order solution (6), (7). Furthermore, we expect the kinetic energy fluctuations to have homogeneous statistics at small scales (where they reside), so that spatial fluxes involving solely fluctuations should be small. We thus expect the balance

$$\partial_y[U \langle v_y^{\omega'} u' \rangle] = \eta - D'. \tag{13}$$

The key difference between Eq. (13) and the analogous balance in 2DNS is in the spatial flux due to the mean flow, preventing a local balance between injection and dissipation. It is this spatial flux which arrests the direct cascade in regions where the mean flow U is strong, carrying the injected kinetic energy away from those regions. By a direct computation using (10), see [19], we find that

$$U \langle v_y^{\omega'} u' \rangle = \partial_y \Psi \langle \partial_y \psi' v_y^{\omega'} \rangle = \eta y. \tag{14}$$

This is confirmed by a direct comparison to DNS in the jet region, Fig. 3(b). Combining (11) and (14) we find that the spatial flux carries all the injected kinetic energy before it has time to cascade to small scales and dissipate there, in agreement with Fig. 3(a).

Conclusion.—We presented results from a perturbative analysis and direct simulations of LQG in the condensate regime, observed here for the first time. Obtaining the two-point correlation functions, we have revealed the different mechanisms determining the odd and even correlators under parity + time reversal. While the former are determined at small scales by a balance between the forcing (breaking time reversal) and the mean flow (breaking parity), the latter are constrained to be zero modes of an advection operator. In fact, this is also the underlying structure in 2DNS [2,9,10], suggesting a universal picture across different 2D flows. We also find an unexpected influence of the mean flow on the direct cascade, which is locally arrested in regions with a strong inverse energy transfer. This phenomenon, absent in 2DNS, is explained by the formation of an out-of-equilibrium spatial flux out of regions where the mean flow is strong. This flux term is a consequence of the locality of the dynamics, and is absent for active scalar models with $m > 0$ and for SWQG with $L_d > l_f$ [19]. It is, however, not ruled out for SWQG with $L_d < l_f$, of which LQG is a limiting case, and it will be interesting to see if a similar expulsion of the direct cascade could be observed there.

*frishman@technion.ac.il

[1] J. Laurie, G. Boffetta, G. Falkovich, I. Kolokolov, and V. Lebedev, Universal profile of the vortex condensate in two-dimensional turbulence, Phys. Rev. Lett. **113**, 254503 (2014).

[2] A. Frishman and C. Herbert, Turbulence statistics in a two-dimensional vortex condensate, Phys. Rev. Lett. **120**, 204505 (2018).

[3] R. H. Kraichnan, Inertial ranges in two-dimensional turbulence, Phys. Fluids **10**, 1417 (1967).

[4] H. Xia, M. Shats, and G. Falkovich, Spectrally condensed turbulence in thin layers, Phys. Fluids **21**, 125101 (2009).

[5] G. K. Vallis, *Atmospheric and Oceanic Fluid Dynamics: Fundamentals and Large-Scale Circulation*, 2nd ed. (Cambridge University Press, Cambridge, England, 2017), 10.1017/9781107588417.

[6] L. M. Smith and V. Yakhot, Bose condensation and small-scale structure generation in a random force driven 2D turbulence, Phys. Rev. Lett. **71**, 352 (1993).

[7] M. Chertkov, C. Connaughton, I. Kolokolov, and V. Lebedev, Dynamics of energy condensation in two-dimensional turbulence, Phys. Rev. Lett. **99**, 084501 (2007).

[8] M. Chertkov, I. Kolokolov, and V. Lebedev, Universal velocity profile for coherent vortices in two-dimensional turbulence, Phys. Rev. E **81**, 015302(R) (2010).

[9] I. V. Kolokolov and V. V. Lebedev, Structure of coherent vortices generated by the inverse cascade of two-dimensional turbulence in a finite box, Phys. Rev. E **93**, 033104 (2016).

[10] A. Frishman, The culmination of an inverse cascade: Mean flow and fluctuations, Phys. Fluids **29**, 125102 (2017).

[11] B. F. Farrell and P. J. Ioannou, Structure and spacing of jets in barotropic turbulence, J. Atmos. Sci. **64**, 3652 (2007).

[12] K. Srinivasan and W. R. Young, Zonostrophic instability, J. Atmos. Sci. **69**, 1633 (2012).

[13] S. M. Tobias and J. B. Marston, Direct statistical simulation of out-of-equilibrium jets, Phys. Rev. Lett. **110**, 104502 (2013).

[14] E. Woillez and F. Bouchet, Theoretical prediction of Reynolds stresses and velocity profiles for barotropic turbulent jets, Europhys. Lett. **118**, 54002 (2017).

[15] E. Woillez and F. Bouchet, Barotropic theory for the velocity profile of Jupiter's turbulent jets: An example for an exact turbulent closure, J. Fluid Mech. **860**, 577 (2019).

[16] V. D. Larichev and J. C. McWilliams, Weakly decaying turbulence in an equivalent-barotropic fluid, Phys. Fluids A **3**, 938 (1991).

[17] J. Marston and S. Tobias, Recent developments in theories of inhomogeneous and anisotropic turbulence, Annu. Rev. Fluid Mech. **55**, 351 (2023).

[18] P. H. Diamond, S.-I. Itoh, K. Itoh, and T. S. Hahm, Zonal flows in plasma—A review, Plasma Phys. Controlled Fusion **47**, R35 (2005).

[19] A. Svirsky, C. Herbert, and A. Frishman, companion paper, Statistics of inhomogeneous turbulence in large-scale quasigeostrophic dynamics, Phys. Rev. E **108**, 065102 (2023).

[20] K. S. Smith, G. Boccaletti, C. C. Henning, I. Marinov, C. Y. Tam, I. M. Held, and G. K. Vallis, Turbulent diffusion in the geostrophic inverse cascade, J. Fluid Mech. **469**, 13 (2002).

[21] R. T. Pierrehumbert, I. M. Held, and K. L. Swanson, Spectra of local and nonlocal two-dimensional turbulence, Chaos Solitons Fractals **4**, 1111 (1994).

[22] A. Venaille, T. Dauxois, and S. Ruffo, Violent relaxation in two-dimensional flows with varying interaction range, Phys. Rev. E **92**, 011001(R) (2015).

[23] K. J. Burns, G. M. Vasil, J. S. Oishi, D. Lecoanet, and B. P. Brown, Dedalus: A flexible framework for numerical simulations with spectral methods, Phys. Rev. Res. **2**, 023068 (2020).

[24] F. Bouchet and E. Simonnet, Random changes of flow topology in two-dimensional and geophysical turbulence, Phys. Rev. Lett. **102**, 094504 (2009).

[25] A. Frishman, J. Laurie, and G. Falkovich, Jets or vortices—What flows are generated by an inverse turbulent cascade?, Phys. Rev. Fluids **2**, 032602(R) (2017).